Astron. Astrophys. 334, 210–220 (1998)

ASTRONOMY AND ASTROPHYSICS

The spin-up of contracting red supergiants

A. Heger[1] **and N. Langer**[2]

[1] Max-Planck-Institut für Astrophysik, Karl-Schwarzschild-Strasse 1, D-85740 Garching, Germany (ahg@mpa-garching.mpg.de)
[2] Institut für Physik, Universität Potsdam, D-14415 Potsdam, Germany (ntl@astro.physik.uni-potsdam.de)

Received 15 January 1998 / Accepted 17 February 1998

Abstract. We report on a mechanism which may lead to a spin-up of the surface of a rotating single star leaving the Hayashi line, which is much stronger than the spin-up expected from the mere contraction of the star.

By analyzing rigidly rotating, convective stellar envelopes, we qualitatively work out the mechanism through which these envelopes may be spun up or down by mass loss through their lower or upper boundary, respectively. We find that the first case describes the situation in retreating convective envelopes, which tend to retain most of the angular momentum while becoming less massive, thereby increasing the specific angular momentum in the convection zone and thus in the layers close to the stellar surface. We explore the spin-up mechanism quantitatively in a stellar evolution calculation of a rotating $12\,\mathrm{M}_\odot$ star, which is found to be spun up to critical rotation after leaving the red supergiant branch.

We discuss implications of this spin-up for the circumstellar matter around several types of stars, i.e., post-AGB stars, B[e] stars, pre-main sequence stars, and, in particular, the progenitor of Supernova 1987A.

Key words: stars: evolution – stars: rotation – circumstellar matter – stars: supergiants – supernovae: individual: SN 1987A

1. Introduction

The circumstellar matter around many stars shows a remarkable axial symmetry. Famous examples comprise Supernova 1987A (Plait et al. 1995; Burrows et al. 1995), the Homunculus nebula around η Carina and other nebulae around so called Luminous Blue Variables (Nota et al. 1995), and many planetary nebulae (Schwarz et al. 1992). A less spectacular example are B[e] stars, blue supergiants showing properties which might be well explained by a circumstellar disk (Gummersbach et al. 1995; Zickgraf et al. 1996). Many of these axisymmetric structures have been explained in terms of interacting winds of rotating stars (cf. Martin & Arnett 1995; Langer et al. 1998; García-Segura et al. 1998), which may be axisymmetric when the stars rotate with a considerable fraction of the break-up rate (Ignace et al. 1996; Owocki et al. 1996). However, up to now only little information is available about the evolution of the surface rotational velocity of stars with time, in particular for their post-main sequence phases.

Single stars which evolve into red giants or supergiants may be subject to a significant spin-down (Endal & Sofia 1979; Pinsonneault et al. 1991). Their radius increases strongly, and if the specific angular momentum were conserved in their surface layers (which may not be the case; see below) they would not only spin down but they would also evolve further away from critical rotation. Moreover, they may lose angular momentum through a stellar wind. Therefore, it may appear doubtful at first whether post-red giant or supergiant single stars can retain enough angular momentum to produce aspherical winds due to rotation.

However, by investigating the evolution of rotating massive single stars, we found that red supergiants, when they evolve off the Hayashi line toward the blue part of the Hertzsprung-Russell (HR) diagram may spin up dramatically, much stronger than expected from local angular momentum conservation. In the next section, we describe the spin-up mechanism and its critical ingredients. In Sect. 3 we present the results of evolutionary calculations for a rotating $12\,\mathrm{M}_\odot$ star, which provides a quantitative example for the spin-up. In Sect. 4 we discuss the relevance of our results for various types of stars, and we present our conclusions in Sect. 5.

2. The spin-up mechanism

2.1. Assumptions

In this paper, we discuss the evolution of the rotation rate of post-main sequence stars, i.e. of stars which possess an active hydrogen burning shell source. This shell source converts hydrogen into helium and thus increases the mass of the helium core with time. However, this takes place on the very long time scale of the thermonuclear evolution of the star, and for the following argument we can consider the shell source as fixed in Lagrangian mass coordinate.

The shell source provides an entropy barrier, which separates the high entropy envelope from the low entropy core, and it marks the location of a strong chemical discontinuity, i.e. a

Send offprint requests to: A. Heger

place of a strong mean molecular weight gradient. Both, the entropy and the mean molecular weight gradient, act to strongly suppress any kind of mixing through the hydrogen burning shell source. This concerns chemical mixing as well as the transport of angular momentum (e.g., Zahn 1974; Langer et al. 1983; Meynet & Maeder 1997). Therefore, in the following, we shall regard the angular momentum evolution of the hydrogen-rich envelopes of the stars under consideration as independent of the core evolution.

This picture is somewhat simplified, as due to the inhibition of angular momentum transport through the shell source the post-main sequence core contraction and envelope expansion results in a large gradient in the angular velocity at the location of the shell source, i.e. a large shear which may limit the inhibiting effects of the entropy and mean molecular weight gradients. However, with the current formulation of shear mixing in our stellar evolution code, we find the angular momentum transport to be insignificant (cf. Sect. 3). In any case, the total amount of angular momentum in the helium core is much smaller than that in the hydrogen-rich envelope ($\lesssim 2\,\%$ in the $12\,\mathrm{M}_\odot$ model discussed below), so that even if all of that would be transported out into the envelope it would not alter its angular momentum balance much.

As a star evolves into a red supergiant, its envelope structure changes from radiative to convective, starting at the surface. If we assume the envelope to be in solid body rotation initially, it can not remain in this state without any transport of angular momentum, unless

$$\frac{\partial \ln i}{\partial m} = \frac{1}{2\pi r^3 \rho} \tag{1}$$

remains constant with time everywhere, i.e. $r^3\rho$ remains constant. Here, m is the Lagrangian mass coordinate, r the radius, ρ the density, and $i = k^2 r^2$ is the specific moment of inertia. For a sphere of radius r the gyration constant is $k^2 = 2/3$, but even for deformed equipotential surfaces of average radius r one still finds k^2 to be of order unity. The assumption that k^2 does not depend on r was used to derive Eq. (1). Obviously, the above homology condition does not hold for stars which change their mode of energy transport in the envelope, since the polytropic index n changes between $n \simeq 3$ in the radiative envelope and $n \simeq 1.5$ in the convective state.

In the following we assume that convection tends to smooth out angular velocity gradients rather than angular momentum gradients, i.e. that convective regions tend to be rigidly rotating. This is certainly a good approximation at least if the rotational period ($P_{\rm rot} = 2\pi/\omega$, where ω is the angular velocity) is long in comparison to the convective time scale ($\tau_{\rm conv} := H_{\rm P}/v_{\rm conv}$, where $v_{\rm conv}$ is the convective velocity and $H_{\rm P}$ is the pressure scale height), and it may also hold for more rapid rotation if convective blobs can be assumed to scatter elastically (cf. Kumar et al. 1995). Latitudinal variations of the rotational velocity as deduced from helioseismological data for the solar convective envelope (Thompson et al. 1996) are not taken into account in our 1D stellar evolution calculation; however, the latitudinal averaged rotation rate of the solar convection zone deviates by no more than $5\,\%$ from solid body rotation (cf. e.g. Antia et al. 1997).

Although, for the considerations in Sect. 2.2 we assume rigid rotation to persist in convection zones, the necessary condition to make the spin-up mechanism described here work is only that convection transports angular momentum on a time scale which is short compared to the evolutionary time scale of the star, and that it leads to a characteristic angular momentum distribution in between the cases of constant angular velocity and constant angular momentum. The efficiency of the spin-up is largest for constant angular velocity and drops to zero for the case of constant angular momentum. The mechanism we present here is not restricted to convection, but any transport of angular momentum that acts towards solid body rotation is suitable to accomplish what we describe here.

2.2. The spin-down of convective envelopes

The rotation frequency of a rigidly rotating convective envelope depends on its moment of inertia and its angular momentum. Both are altered by mass loss from this envelope, the former by loss of mass, the latter by the accompanied loss of angular momentum. Additionally, the envelope's moment of inertia is also affected by changes of its density stratification.

Here, we want to discuss two processes which can change the rotation frequency of a rigidly rotating convective envelope without employing global contraction or expansion of the star, but rather by mass outflow through its upper or lower boundary. We will show that the first case leads to a spin-down, while the latter spins the envelope up.

The spin-down of mass losing rigidly rotating envelopes can be understood by breaking up the continuous mass and angular momentum loss into three discrete steps (see the left hand side of Fig. 1, cf. also Langer 1998), neglecting secular changes of the stellar structure. Starting from a rigidly rotating envelope extending from $R_{\rm c}$ to R_0 (A1), the outer part of the convective envelope located between R_1 and R_0 is removed by stellar mass loss within the time interval Δt (A1 $\rightarrow$ A2). In the second step, for which we assume local angular momentum conservation, the envelope re-expands to roughly its original size (A2 $\rightarrow$ A3). This results in a slow-down of the surface rotation and, as the layers deep inside the envelope expand less, differential rotation below (A3). In the third step, rigid rotation is re-established by an upward transport of angular momentum (A3 $\rightarrow$ A4). As this implies an averaging of the angular velocity, it is clear from Fig 1 (A4) that now the whole convective envelope rotates slower than at the beginning of step 1. Obviously, the redistribution of angular momentum towards the stellar surface leads to an increase of the angular momentum loss rate.

The efficiency of the angular momentum loss induced by mass loss from the surface of a rigidly rotating envelope, i.e. the amount of angular momentum lost per unit mass lost relative to

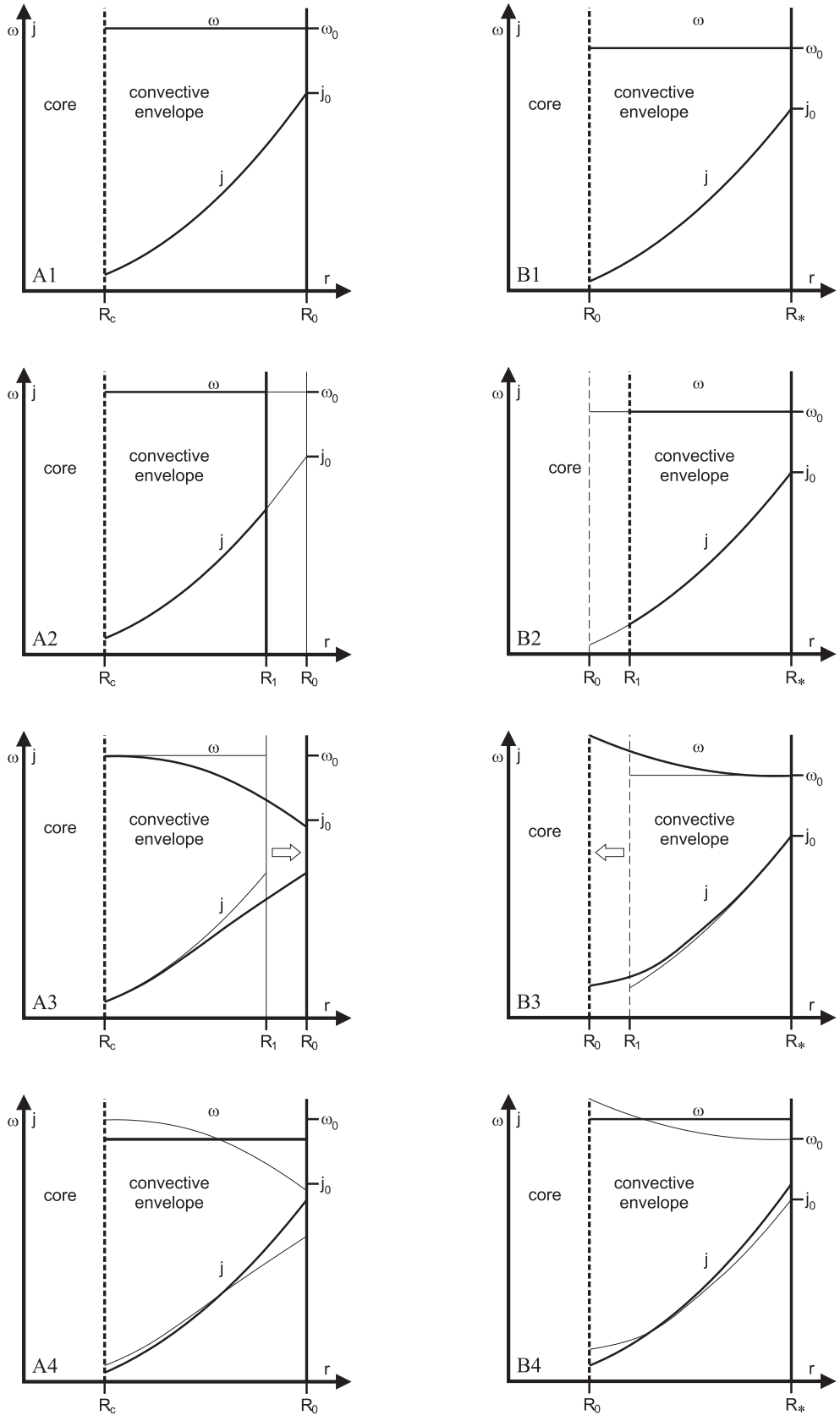

Fig. 1. Mass loss from a rigidly rotating stellar envelope from the surface (case A: left panels) and through its lower boundary (case B: right panels). For illustration, the continuous process is split up into three steps. First (panels $1 \rightarrow 2$), mass is removed from the envelope, second, the envelope restores its original radial extent through expansion (panels $2 \rightarrow 3$), and third (panels $3 \rightarrow 4$), the angular momentum is redistributed such that rigid rotation is restored. It leads to spin-down (spin-up) and decrease (increase) of the specific angular momentum for the case of mass loss trough the upper (lower) boundary of the convective envelope. Thin lines show the state of the preceding step.

average specific angular momentum of the envelope, is given by

$$\chi := \frac{\dot{J}}{\dot{M}} \frac{M_{\rm env}}{J_{\rm env}} = \frac{j_{\rm surf}}{\langle j \rangle_{\rm env}} = \frac{i_{\rm surf}}{\langle i \rangle_{\rm env}} \approx \frac{{R_\star}^2}{\langle r^2 \rangle_{\rm env}} \ , \qquad (2)$$

where $M_{\rm env}$ and $J_{\rm env}$ are total mass and total angular momentum of the envelope, $\dot{M}$ and $\dot{J}$ are stellar mass and angular momentum loss rate, $j_{\rm surf}$ and $i_{\rm surf}$ are the specific angular momentum and moment of inertia at the surface, respectively, and $R_\star$ is the stellar radius. The mean value of a quantity x over the envelope is defined by

$$\langle x \rangle_{\rm env} := \frac{1}{M_{\rm env}} \int_{M-M_{\rm env}}^{M} x(m)\, {\rm d}m \ ,$$

where M is the mass of the star. The larger χ the more efficient is the loss of angular momentum per unit mass lost. A value of $\chi > 1$ corresponds to a decrease of the mean specific angular momentum of the envelope, $\chi < 1$ to an increase. For the case of mass loss from the surface of a rigidly rotating stellar envelope χ is always greater than 1.

The density stratification in the envelope determines how much angular momentum is stored in the layers close to the surface relative to the total angular momentum of the envelope. An envelope structure which holds most of the mass close to its bottom favors high angular momentum loss rates, since this decreases $\langle r^2 \rangle_{\rm env}$. In red supergiants, on the other hand, $\langle r^2 \rangle_{\rm env}$ is rather high, since those stars store a large fraction of their mass in layers far from the stellar center, thus reducing χ.

This is demonstrated in Fig. 2, where we plotted the moment of inertia per unit radius, ${\rm d}I(r)/{\rm d}r = 8\pi r^4 \rho/3$ for spherical symmetry, as a function of the fractional radius for different types of stars. For a red supergiant model with extended convective envelope we find the major contribution to the total moment of inertia I of the star at radii around $\sim 2/3\, R_\star$ ($\chi \approx 9/4$), whereas for the zero-age main sequence (ZAMS) model matter at $\sim 1/3\, R_\star$ dominates the moment of inertia of the star ($\chi \approx 9$). As main sequence stars can be approximated by rigid rotators (cf. Zahn 1994), the whole star takes the rôle of the stellar envelope as far as our definition of χ is concerned. Therefore, the considered main sequence star loses its angular momentum four times more efficient than the red supergiant model plotted in Fig. 2.

Two other cases are shown in Fig. 2, i.e., a red supergiant model shortly before its transition into the blue supergiant stage, where I is dominated by the density inversion at the upper edge of the convective region, making the angular momentum loss from the envelope of this star quite inefficient ($\chi \approx 1.5$), and a blue supergiant model during central helium burning in which the moment of inertia is concentrated even more towards the center of the star ($\chi \approx 30$) than for the ZAMS model. Thus, if the envelopes of blue supergiants stay close to solid body rotation — which is indicated by our time-dependent calculations — they experience a more efficient spin-down than main sequence stars.

However, since for blue supergiants the total moment of inertia I is smaller than for their progenitor main sequence stars,

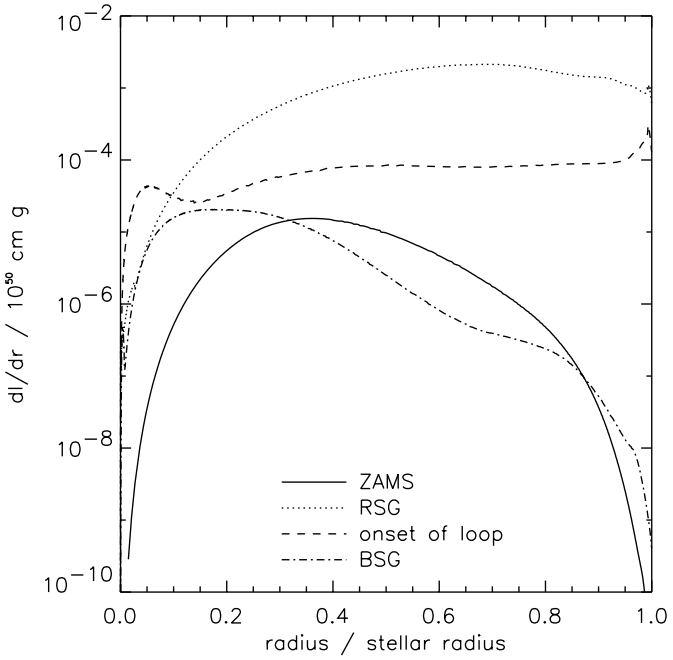

Fig. 2. Moment of inertia per radius ${\rm d}I(r)/{\rm d}r$ as a function of radius (in units of the stellar radius) for four different stellar models. The solid line shows a ZAMS model, the dotted line a red supergiant model with an almost fully convective hydrogen-rich envelope, the dashed line a red supergiant model just before the blue loop, and the dash-dotted line a blue supergiant during the blue loop. All models are taken from the $12\,{\rm M}_\odot$ sequence described in detail below.

they may get closer to critical rotation (cf. Sect. 3.1) if they keep their angular momentum. This may be in particular the case for metal poor massive stars. Those have much smaller mass loss and therefore angular momentum loss rates, and they can evolve from the main sequence directly into a long-lasting blue supergiant stage without an intermediate red supergiant phase (cf. e.g. Schaller et al. 1992); we found such stars to obtain critical rotation as blue supergiants in preliminary evolutionary calculations.

2.3. The spin-up of convective envelopes

The spin-up of convective envelopes which decrease in mass due to an outflow through their *lower* boundary is understood in a similar way to the mass loss process discussed above. Again we want to split up this process into three discrete steps (see sequence B on the right hand side of Fig. 1). Starting from a rigidly rotating envelope extending from R_0 to $R_\star$ (B1), the inner part of the convective envelope, located between R_0 and R_1, becomes radiative within some time Δt (B2). Then the envelope re-expands to its original size. As local angular momentum conservation is assumed in this step, it results in a spin-up of most of the convective envelope, which is weaker for the layers farther out. The outcome is a differentially rotating envelope which spins fastest at its bottom (B3). Since the envelope has to go back to rigid rotation, angular momentum is transported upward in the next step until this is achieved (B4). We end up

with higher specific angular momentum in the whole convective envelope compared to the initial configuration.

As can be seen in Fig. 5 below, during the evolution of a red supergiant towards the blue part of the HR diagram the radial extent of the convective envelope remains about fixed while mass shells drop out of the convective region. If one imagines the convective envelope to consist of moving mass elements or blobs, the spin-up process can thus also be understood as follows. A blob, starting somewhere in the convective region will, as it approaches the lower edge of the convective envelope, decrease its specific moment of inertia and therefore has to lose angular momentum in order to remain in solid body rotation with the whole convective region. Angular momentum has to be transferred to rising blobs such that also they remain in solid body rotation. Mass elements leaving the convective envelope thus only remove small amounts of angular momentum from the convective region. Therefore, the average specific angular momentum of the remaining convective envelope will increase and thus it spins up.

Replacing $j_{\rm surf}$, $i_{\rm surf}$ and $R_\star$ in Eq. (2) by $j_{\rm low}$, $i_{\rm low}$ and $R_{\rm low}$, the specific angular momentum, the specific moment of inertia and the radius at the lower edge of the convective envelope, respectively, one can define an efficiency of angular momentum loss through the lower boundary, $\tilde{\chi}$. We find $\tilde{\chi} \ll 1$, especially for those cases where χ is small, as e.g. for the red supergiant envelopes under consideration here.

The total change of specific angular momentum of the envelope $\langle j \rangle_{\rm env}$ by mass loss through the upper and lower boundary can then be written as

$$\frac{{\rm d} \ln \langle j \rangle_{\rm env}}{{\rm d}t} = \frac{\dot{M}\,(1-\chi) + \dot{M}_{\rm low}\,(1-\tilde{\chi})}{M_{\rm env}}\ , \qquad (3)$$

where $\dot{M}_{\rm low}$ is the rate at which mass leaves the envelope through its lower boundary. For our sample calculation it is $\tilde{\chi} \ll 1$, χ of order unity, and $\dot{M} \ll \dot{M}_{\rm low}$ during the red supergiant stage preceding the evolution off the Hayashi line, so that $\langle j \rangle_{\rm env}$ almost increases as $M_{\rm env}$ decreases,

$${\rm d} \ln \langle j \rangle_{\rm env} / {\rm d} \ln M_{\rm env} \gtrsim -1\ ,$$

reflecting the fact that angular momentum does not get lost efficiently from the convective envelope through its upper nor its lower boundary. The approximation $\tilde{\chi} \ll 1$ is hardly affected by the variation of the lower bondary radius seen in Fig. 5. Thus, the convective envelope loses most of its mass but keeps a major part of the angular momentum.

When the convective envelope gets depleted in mass and the stellar radius decreases considerably, the global contraction of the stellar envelope results in an additional contribution to its spin-up. Still, mass elements drop out of the convective region (cf. Fig. 5), but now the contraction leads to an increase of the rotation velocity, and the star can reach rotation velocities of the order of the break-up velocity (see below). However, the contraction does not contribute to the increase of the specific angular momentum at the surface.

Finally, we want to note that if the whole star would remain rigidly rotating, e.g., due to the action of magnetic fields inside the star or by more efficient shear instabilities, its spin-up would occur very similar to the case described here. In that case, also mass shells from the core would transfer part of their angular momentum to layers above, which would make the spin-up somewhat more efficient. However, since in a red supergiant the mass elements lose the major part of their angular momentum to the convective envelope before they leave it, and the amount of angular momentum contained in the core is small anyway (cf. Sect. 2.1), the additional spin-up will be small (cf. Fig. 7 before blue loop).

3. Numerical simulations

3.1. Input physics

The stellar evolution calculations presented here are obtained with an implicit hydrodynamic stellar evolution code (cf. Langer et al. 1988). Convection according to the Ledoux criterion and semiconvection are treated according to Langer et al. (1983), using a mixing length parameter $\alpha_{\rm MLT} = 1.5$ and semiconvective mixing parameter of $\alpha_{\rm sem} = 0.04$ (Langer 1991a). Opacities are taken from Alexander (1994) for the low temperature regime, and from Iglesias et al. (1996) for higher temperatures. The effects of rotation on the stellar structure as well as the rotationally induced mixing processes are included as in Pinsonneault et al. (1989), with uncertain mixing efficiencies adjusted so as to obtain a slight chemical enrichment at the surface of massive main sequence stars (cf. Fliegner et al. 1996).

The mass loss rate was parameterized according to Nieuwenhuijzen & de Jager (1990), but modified for a rotationally induced enhancement of mass loss as the star approaches the Ω-Limit (cf. Langer 1997), i.e.

$$\frac{\dot{M}(\omega)}{\dot{M}(\omega=0)} = \left(\frac{1}{1-\Omega}\right)^{0.43}$$

(cf. Friend & Abbott 1986) where

$$\Omega := \frac{\omega}{\omega_{\rm c}}\ , \quad \omega_{\rm c} := \sqrt{\frac{Gm}{r^3}\,(1-\Gamma)}\ , \quad \Gamma := \frac{\kappa L}{4\pi c G M}\ .$$

Here, κ is the Rosseland opacity. Γ is not only evaluated at the stellar surface, but its maximum value in the radiative part of the optical depth range $\tau \in [2/3, 100]$ (cf. Lamers 1993; Langer 1997) is used.

The quantitative result for the Ω-dependence of the mass loss rate obtained by Friend & Abbott (1986) was questioned by Owocki et al. (1996), who performed hydrodynamic simulations of winds of rotating hot stars including the effect of non-radial radiation forces and gravity-darkening in the way described by von Zeipel (1924). However, the only crucial ingredient for the model calculations, which is confirmed by Owocki et al. (1997), is the fact that the mass loss rate increases strongly as the star approaches the Ω-limit, so that the star cannot exceed critical rotation, but rather loses more mass and angular momentum (cf. also Langer 1998).

To quantify the angular momentum loss due to stellar winds, $\dot{J}$, we assume that, at any given time, the mean specific angular momentum of the wind material leaving the star equals the

specific angular momentum averaged over the rigidly rotating, spherical stellar surface, which we designate as $j_{\rm surf}$.

The transport of angular momentum inside the star is modeled as a diffusive process according to

$$\frac{\partial \omega}{\partial t} = \frac{1}{4\pi r^2 \rho i} \frac{\partial}{\partial r} \left[4\pi r^2 \rho i D \frac{\partial \omega}{\partial r} \right] - \dot{r} \left(\frac{\partial \omega}{\partial r} + \omega \frac{\partial \ln i}{\partial r} \right),$$

where D is the diffusion coefficient for angular momentum transport due to convection and rotationally induced instabilities (cf. Endal & Sofia 1979; Pinsonneault et al. 1991), and the last term on the right hand side accounts for advection. The diffusion equation is solved for the whole stellar interior. In stable layers, the diffusion coefficient is zero. We specify boundary conditions at the stellar surface and the stellar center which guarantee angular momentum conservation to numerical precision.

Our prescription of angular momentum transport yields rigid rotation when and wherever the time scale of angular momentum transport is short compared to the local evolution time scale, no matter whether rotationally induced mixing or convective mixing processes are responsible for the transport. Chaboyer & Zahn (1992) found that meridional circulations may lead to advection terms in the angular momentum transport equation, which may have some influence on the evolution of the angular momentum distribution in the stellar envelope during the main sequence phase (cf. Talon et al. 1997). However, the omission of these terms has no consequences for the spin-up process describe here, since it is dominated by the much faster angular momentum transport due to convection. Since the time scale of convection is generally much smaller than the evolution time, convective regions are mostly rigidly rotating in our models.

The effect of instabilities other than convection on the transport of matter and angular momentum are of no relevance for the conclusions obtained in the present paper. E.g., mean molecular weight gradients have no effect on the spin-up process described below since it occurs in a retreating convection zone (see below).

Calculations performed with a version of the stellar evolution code KEPLER (Weaver et al. 1978), which was modified to include angular momentum, confirm the spin-up effect obtained with our code which is described in Sect. 3.2.

3.2. Results

We have computed stellar model sequences for different initial masses and compositions (cf. Heger et al. 1997), but here we focus on the calculation of a $12\,{\rm M}_\odot$ star of solar metallicity. This simulation is started on the pre-main sequence with a fully convective, rigidly rotating, chemically homogeneous model consisting of $28\,\%$ helium and $70\,\%$ hydrogen by mass and a distribution of metals with relative ratios according to Grevesse & Noels (1993). Its initial angular momentum of $110\,10^{50}\,{\rm erg\,s}$ leads to an equatorial rotation velocity of $\sim 200\,{\rm km\,s^{-1}}$ on the main sequence, which is typical for these stars (cf. Fukuda 1982; Halbedel 1996).

During the main sequence evolution the star loses $25\,\%$ of its initial angular momentum and $0.23\,{\rm M}_\odot$ of its envelope due to stellar winds. After the end of central hydrogen burning, the star settles on the red supergiant branch after several $10^4\,{\rm yr}$ and develops a convective envelope of $8.3\,{\rm M}_\odot$. During this phase it experiences noticeable mass loss ($\dot{M} \approx 8\,10^{-7}\,{\rm M}_\odot\,{\rm yr}^{-1}$), but the angular momentum loss per unit mass lost $\dot{J}/\dot{M} \approx 1.7\,10^{19}\,{\rm cm^2\,s^{-1}}$ is lower than on the main sequence (cf. Sect. 2.2).

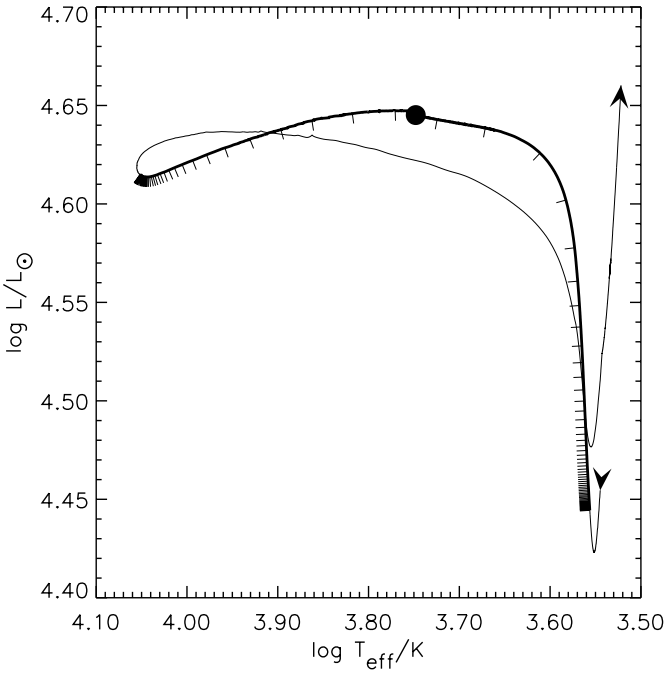

Fig. 3. Track of the $12\,{\rm M}_\odot$ star in the HR diagram during its blue loop. The two arrows indicate the direction of the evolution. The thick drawn part of the track corresponds to the time span shown in Figs. 6 and 7. The star spends $1\,000\,{\rm yr}$ between two neighboring tick marks. The thick dot indicates where the star obtains its maximum mass and angular momentum loss rates; see the dotted line in Fig. 6.

Shortly after core helium ignition, the bottom of the convective envelope starts to slowly move up in mass. About $4\,10^5\,{\rm yr}$ later (at a central helium mass fraction of $65\,\%$), the convective envelope mass decreases more rapidly. After another $\sim 5\,10^5\,{\rm yr}$ it reaches a value of $\sim 3\,{\rm M}_\odot$. Up to this time, the star has lost $0.75\,{\rm M}_\odot$ as a red supergiant, and $43\,\%$ of the angular momentum left at the end of the main sequence.

At its largest extent in mass, the convective envelope contains a total angular momentum of $77\,10^{50}\,{\rm erg\,s}$, of which $17\,10^{50}\,{\rm erg\,s}$ are contained in the lower $4.5\,{\rm M}_\odot$. After those layers dropped out of the convective envelope, they have kept only $2.8\,10^{50}\,{\rm erg\,s}$ whereas $44\,10^{50}\,{\rm erg\,s}$ remain in the convective envelope; $30\,10^{50}\,{\rm erg\,s}$ have been lost due to mass loss. Thus, on average the specific angular momentum of the lower part of the convective envelope is decreased by up to a factor of ~ 5, while that of the remaining convective envelope increased on average by a factor of 1.5, despite the angular momentum loss from the surface (cf. Fig. 4, Eq. (3)). For comparison, the helium core contains never more than $\sim 1.5\,10^{50}\,{\rm erg\,s}$.

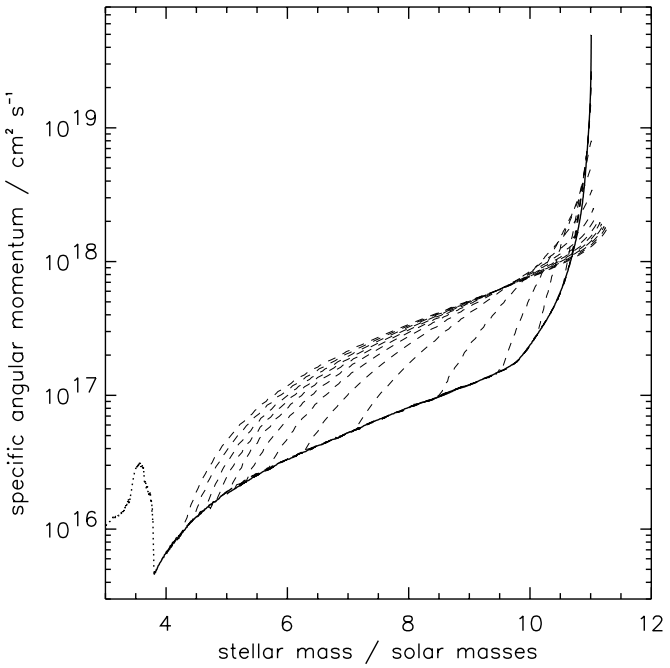

Fig. 4. Evolution of the internal specific angular momentum profile in the hydrogen-rich envelope of the $12\,\mathrm{M}_\odot$ sequence during the first part of core helium burning which is spent as a red supergiant. Dashed lines show specific angular momentum versus mass coordinate in the convective part of the envelope for different times, from $420\,000\,\mathrm{yr}$ to $2\,000\,\mathrm{yr}$ before the red $\rightarrow$ blue transition, with those reaching down to lower mass coordinates corresponding to earlier times and extending to higher mass coordinates, because the stellar mass decreases with time. The solid line shows the angular momentum profile for those mass zones which have dropped out of the convective envelope, which remains frozen in later on. The dotted line marks the angular momentum profile in the inner stellar region which is never part of the convective envelope.

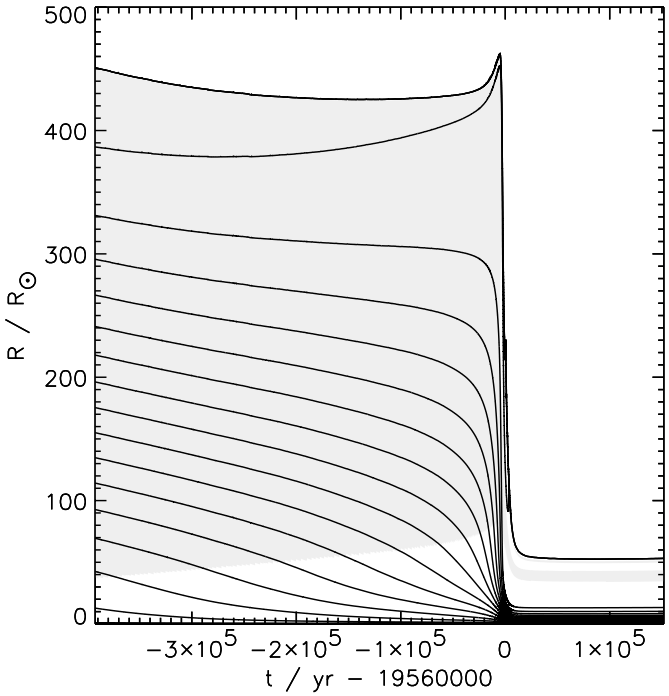

Fig. 5. Evolution of the radii of different mass shells as a function of time for a period including the transition from the red to the blue supergiant stage of the $12\,\mathrm{M}_\odot$ model. The zero-point on the x-axis corresponds to the thick dot in Fig. 3 and corresponds roughly to the time of the red $\rightarrow$ blue transition. Except for the uppermost solid line, which corresponds to the surface of the star, the lines trace Lagrangian mass coordinates. The mass difference between the lines is $0.5\,\mathrm{M}_\odot$. Shading indicates convective regions.

At this point of evolution, the transition to the blue sets in in our model. Within the next $\sim 25\,000\,\mathrm{yr}$ another $2\,\mathrm{M}_\odot$ drop out of the convective envelope which then comprises only about $1\,\mathrm{M}_\odot$ but has still the full radial extent of a red supergiant. The ensuing evolution from the Hayashi line to the blue supergiant stage takes about $10\,000\,\mathrm{yr}$ (cf. Fig. 3). During this time, the angular momentum transport to the outermost layers of the star continues, tapping the angular momentum of those layers which drop out of the convective envelope.

The contraction of the star by a factor of $f \approx 10$ (cf. Fig. 5) reduces the specific moment of inertia at the surface by $f^2 \approx 100$ and ω would be increased by the same factor if j were conserved locally. This would imply an increase of the equatorial rotational velocity by a factor of ~ 10 (cf. Fig. 7, "decoupled"). The true increase in the rotational velocity is one order of magnitude larger, due to the spin-up effect described in Sect. 2, and it would be even larger if the star would not arrive at the Ω-limit (see Fig. 7) and lose mass and angular momentum at an enhanced rate.

For local angular momentum conservation Ω scales as $\Omega \propto 1/\sqrt{R(1-\Gamma)}$. A value of $\Gamma \approx 2\,10^{-3}$ is found on the red supergiant branch in our calculation, and $\Gamma \approx 0.4$ for the blue supergiant stage. This by itself would increase Ω by a factor of ~ 3.9 during the red $\rightarrow$ blue transition. Actually, Ω changes from ≈ 0.01 at the red supergiant branch at the beginning of central helium burning to $\Omega \approx 1$ — to critical rotation — at the red $\rightarrow$ blue transition, i.e. by a factor ~ 100, despite significant mass and angular momentum loss.

At an effective temperature of $\sim 6\,000\,\mathrm{K}$ the Eddington-factor Γ at the surface (as defined above) rises from a few times 10^{-3} to ~ 0.4, mainly due to an increase in the opacity; the luminosity remains about constant. Around $40\,\%$ of the angular momentum of the star are then concentrated in the upper $0.01\,\mathrm{M}_\odot$. Since Ω becomes close to 1, the mass loss rate rises to values as high as several $10^{-5}\,\mathrm{M}_\odot\,\mathrm{yr}^{-1}$ (cf. Fig. 6) in order to keep the star below critical rotation, with the result that these layer are lost within a few $1\,000\,\mathrm{yr}$. This is by far the most dramatic loss of angular momentum, i.e. the highest value of $\dot{J}$, the star ever experiences. The specific angular momentum loss $\dot{J}/\dot{M}$ reaches a peak value of $7.7\,10^{19}\,\mathrm{cm}^2\,\mathrm{s}^{-1}$ (cf. Fig. 6).

After arriving at the blue supergiant stage, the star still experiences a high angular momentum loss rate for some time, since the major part of the star's angular momentum is still concentrated in the vicinity of the surface. Interestingly, the star now even spins faster than when rigid rotation of the whole star were assumed (cf. Fig. 7), because within the blue supergiant's

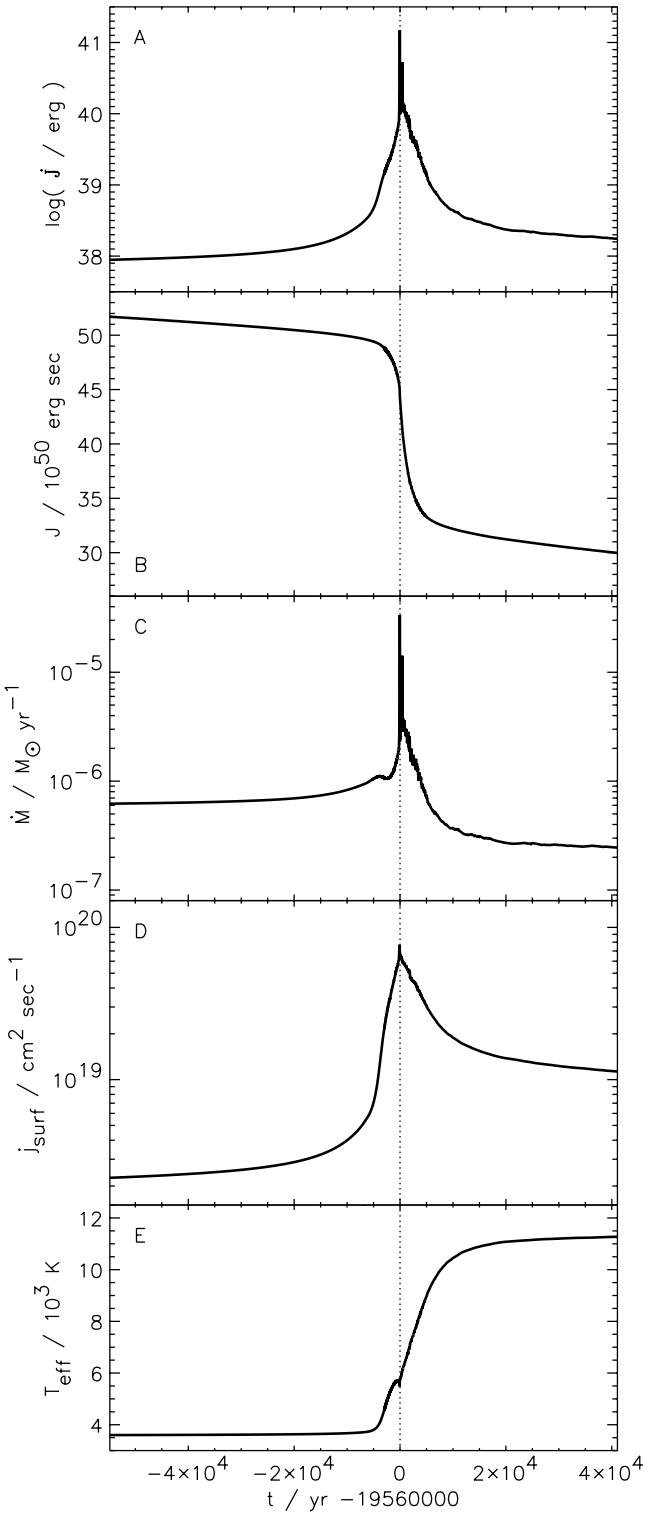

Fig. 6. Evolution of characteristic stellar properties as function of time, during the first part of the blue loop of our $12\,\mathrm{M}_\odot$ model (cf. Fig. 3). The time zero-point is defined as in Fig. 5 and is marked by the dotted line. Displayed are: the angular momentum loss rate $\dot{J}$ (**A**), the total angular momentum J (**B**), the mass loss rate $\dot{M}$ (**C**), the specific angular momentum loss rate $j_{\rm surf} = \dot{J}/\dot{M}$ (**D**), and the effective temperature $T_{\rm eff}$ (**E**).

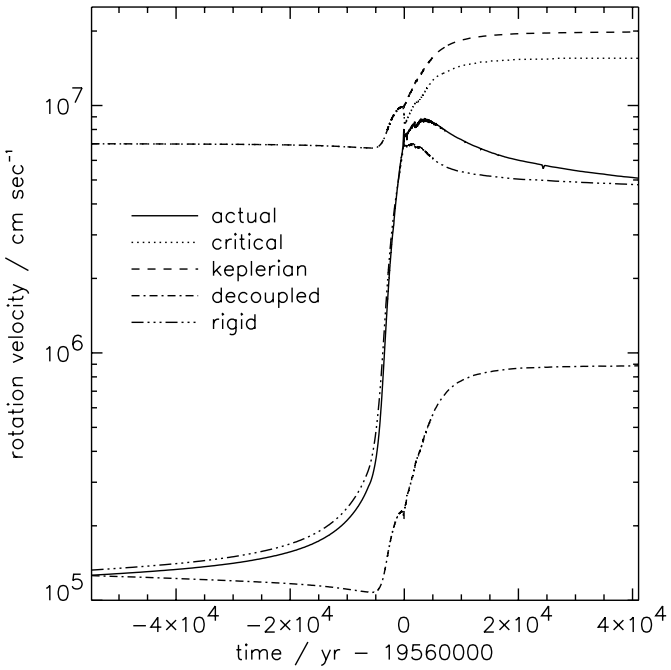

Fig. 7. Equatorial rotation velocity as function of time (solid line) compared to the Keplerian (dashed line) and the critical (dotted line) rotation rate; the latter two are different by the factor $\sqrt{1-\Gamma}$. During the red supergiant phase it is $\Gamma \ll 1$ and the two lines coincide, while during the blue supergiant phase Γ rises to 0.4. The dash-dotted line shows the evolution of the surface rotation rate if there were no angular momentum transport in the convective envelope, and the dash-triple-dotted line shows how the surface rotation rate would evolve if the whole star would maintain rigid rotation.

radiative envelope the angular momentum is not transported downward efficiently. However, due to mass loss, this deviation does not persist long.

Due to the long duration of the blue supergiant phase, several 10^5 yr in comparison to the 10^4 yr the red $\rightarrow$ blue transition takes, the total angular momentum J is reduced by another factor ~ 3 although both, the mass and the angular momentum loss rate, become smaller with time. In total, after the blue loop the star has ~ 5 times less angular momentum than before, and thus red supergiants which underwent a blue loop rotate significantly slower than those which did not.

4. Discussion

The mechanism to spin-up stellar envelopes presented above enhances the specific angular momentum in the surface layers of the star by some factor (cf. Sect. 3.2); a question to be considered separately is the origin of the angular momentum, and also in which cases critical rotation is reached. For single stars, the available angular momentum seems to be limited to that of the ZAMS star, reduced by the angular momentum lost during its evolution. A way to supply a considerable amount of angular momentum to the star would be the capture of a companion star or planet (Soker 1996; Podsiadlowski 1998). This might occur when the star first becomes a red supergiant. The resulting

configuration would have a much higher angular momentum than a normal single star, but still, due to the high moment of inertia of the supergiant, it could initially be far away from critical rotation. Due to the spin-up mechanism described here, such a star might then approach critical rotation even before the transition into a blue supergiant.

The mechanism to spin-up stellar envelopes (Sect. 2), which was applied to a post-red supergiant $12\,\mathrm{M}_\odot$ star in Sect. 3, may operate in all evolutionary phases during which stars evolve from the Hayashi-line towards the hotter part of the HR diagram. These comprise the transition of pre-main sequence stars form their fully convective stage to the main sequence, the transition of low and intermediate mass stars from the Asymptotic Giant Branch (AGB) to central stars of planetary nebulae, the blue loops of stars in the initial mass range $\sim 3\,\mathrm{M}_\odot ... \sim 25\,\mathrm{M}_\odot$, and the transition of massive red supergiants into Wolf-Rayet (WR) stars. For all four phases, observational evidence for axisymmetric circumstellar matter exists.

A high value of Ω during the evolution off the Hayashi line can be expected to have notable influence not only on the mass and angular momentum loss rate as in the case studied in Sect. 3, but also on the geometry of the wind flow. At present, theoretical predictions of the latitudinal dependence of stellar wind properties for rapidly rotating stars are ambiguous. Bjorkman & Cassinelli (1993) have proposed that angular momentum conservation of particles in a pressure free wind which is driven by purely radial forces leads, for sufficiently large values of Ω, to high ratios of equatorial to polar wind density, i.e. to disks or disk-like configurations. Owocki et al. (1996) found that this might no longer be the case when the non-radial forces occurring in hot star winds are accounted for. For cooler stars, the prospects of disk formation may thus be better (cf. also Ignace et al., 1996). To discuss the geometry of the winds of our models is beyond the scope of this paper; however, we want to point out that the maximum values of Ω and $\dot{J}/\dot{M}$ occur at about $T_{\rm eff} \simeq 6\,000\,\mathrm{K}$ (cf. Sect. 3.2 and Fig. 6), so that an equator-to-pole wind density ratio larger than one may still be justified.

4.1. Blue loops during or after core helium burning

An interesting example where the spin-up mechanism described in this paper should almost certainly have played a rôle is the progenitor of SN 1987A. In fact, the SN 1987A progenitor is the only star of which we are reasonably sure that it performed a blue loop, in this case after core helium exhaustion (cf. Arnett et al. 1989)

The structures observed around SN 1987A seem to be rotationally symmetric with a common symmetry axis, which may suggest that rotation has played a major rôle in their formation. The inner of the three rings is currently explained by the interaction of the blue supergiant wind with the wind of the red supergiant precursor (cf., Chevalier 1996). However, this interaction would result in a spherical shell in case of spherically symmetric winds. To understand the ring structure of the inner interaction region, and maybe also the two outer rings, significant rotation appears therefore to be required (cf. Martin & Arnett 1995), which may be provided by our spin-up mechanism. We may note that for this mechanism to work it is insignificant what actually triggered the blue loop; i.e. it would work as well for single star scenarios with a final blue loop (cf. Langer 1991b; Meyer 1997; Woosley et al. 1998) or for binary merger scenarios which predict a final red $\rightarrow$ blue transition of the merger star (cf. Podsiadlowski 1998).

We do not expect to find ring nebulae frequently around blue supergiants (cf. Brandner et al. 1997), since the time scale on which our model (cf. Sect. 3) shows very high surface rotation rates is rather small compared to the typical life time of a blue supergiant (cf. Langer 1991a), and because they are quickly dissolved by the blue supergiant wind. SN 1987A is an exception, since here the transition to the blue happened only short time ago (i.e. the supernova exploded only shortly after the transition). However, a certain type of B supergiants, the B[e] stars, show emission line features which might be due to a circumstellar disk (cf. Zickgraf et al. 1996). The location of the less luminous subgroup of B[e] stars in the HR diagram (Gummersbach et al. 1995) is in fact consistent with a blue loop scenario for their evolution. I.e., their disks might be produced by the spin-up mechanism described here (cf. also Langer & Heger 1998).

4.2. Red supergiant $\rightarrow$ Wolf-Rayet star transition

The transition of massive mass losing red supergiants into Wolf-Rayet stars is the massive star analogue of the AGB $\rightarrow$ post-AGB star transition. It occurs when the mass of the hydrogen-rich envelope is reduced below a critical value (cf., e.g., Schaller et al. 1992) and should not be confused with the blue loops discussed in Sect. 4.1. As in the post-AGB case (Sect. 4.4), the spin-up mechanism can be expected to work. Unlike in the case discussed in Sect. 3.2, the major part of the envelope is lost due to stellar winds before the red supergiant $\rightarrow$ Wolf-Rayet star transition, with the consequence of considerable angular momentum loss. Therefore, it may be more difficult for the star to reach critical rotation during the contraction.

However, there are signs of asphericity in the ring nebula NGC 6888 around the Galactic Wolf-Rayet star WR 136 which has been interpreted as swept-up red supergiant wind shell by García-Segura & Mac Low (1995) and García-Segura et al. (1996). Also, Oudmaijer et al. (1994) report on bi-polar outflows from IRC+10420, a massive star just undergoing the red-supergiant $\rightarrow$ Wolf-Rayet star transition. IRC+10420 is currently an F type star, i.e. it has an effective temperature at which we expect the maximum effect of the spin-up mechanism discussed here (cf. Sect. 3.2). Therefore, in the absence of a binary companion, the spin-up mechanism may yield the most promising explanation for the bipolar flows.

4.3. Pre-main sequence evolution

As mentioned in Sect. 3.2, we started our $12\,\mathrm{M}_\odot$ sequence from a fully convective pre-main sequence configuration. We expected the spin-up mechanism found for the post-red supergiant stage to be also present in the contraction phase towards the

main sequence. An analysis of this evolutionary phase showed in fact its presence, although the efficiency of the spin-up was found to be somewhat smaller. During that part of the pre-main sequence contraction phase where the convective region retreats from the center of the star to its surface, the star would have increased its equatorial rotational velocity by a factor of ~ 3 if angular momentum were conserved locally, but it was spun-up by a factor of ~ 10. I.e., the spin-up mechanism described in Sect. 2 resulted in an additional increase of the rotational velocity of a factor of ~ 3. This was not enough to bring the star to critical rotation in this phase. However, if the initial rotation rate would have been larger, a phase of critical rotation during the pre-main sequence stage would well be possible.

While a fully convective pre-main sequence stage may not be realistic for massive stars and is just assumed in our case for mathematical convenience, pre-main sequence stars of low and intermediate mass are supposed to evolve through a fully convective stage (Palla & Stahler 1991). During the transition from this stage to the main sequence, the spin-up mechanism described in this paper might operate. Pre-main sequence stars in the corresponding phase, i.e. past the fully convective stage but prior to core hydrogen ignition, are often found to have disks. They correspond to the T Tauri stars at low mass (e.g., Koerner & Sargent 1995) and to central stars of Herbig Haro objects at intermediate mass (e.g., Marti et al. 1993). However, the disks are usually interpreted as remnants of the accretion process which built up the star. Since pre-main sequence stars are often found to be rapid rotators (cf. Walker 1990), we may speculate here about a possible contribution to the disk due to decretion from the star reaching critical rotation due to spin-up (cf. Krishnamurtihi et al. 1997).

4.4. Post-AGB evolution

Low and intermediate mass stars leave the AGB when the mass of their hydrogen-rich envelope decreases below a certain value. When this happens, the envelope deflates, the stellar radius decreases, and the energy transport in the envelope changes from convective to radiative. The spin-up mechanism described in Sect. 2 can be expected to operate in this situation, as in the red supergiant $\rightarrow$ Wolf-Rayet star transition (Sect. 4.2).

Whether or not post-AGB stars can reach critical rotation due to this spin-up is not clear. Certainly, the heavy mass loss during the evolution on the AGB spins the envelope down according to the mechanism sketched in Fig. 1. The ratio of the rotation rate to the critical rotation rate Ω may be further affected by random kicks due to asymmetric mass loss, which may keep the envelope at some level of rotation (cf. Spruit 1998), or by transport of angular momentum from the core to the envelope, which may be efficient during the thermal pulses, and by the evolution of the critical rotation rate, which depends on the Eddington factor Γ and thereby on the opacity coefficient (cf. García-Segura et al. 1998).

Clearly, the spin-up mechanism described in this paper may help to bring post-AGB stars — or more specific: stars which just left the AGB, i.e. central stars of proto-planetary nebulae — closer to critical rotation. It may play a rôle in explaining axisymmetric flows which are often observed in central stars of proto-planetary nebulae (cf. Kwok 1993) and the shapes of bi-polar planetary nebulae (cf. Schwarz et al. 1993; Stanghellini et al. 1993; García-Segura et al. 1998).

5. Summary and conclusions

In this paper, we discussed the effect of mass outflow through the inner or outer boundary of a rigidly rotating envelope on its rotation frequency. It causes a change of the specific angular momentum in the envelope and alters its rotation rate besides what results from contraction or expansion (cf. Fig. 7). For constant upper and lower boundaries of the envelope, which we found a good approximation for convective envelopes (cf. Fig. 5), a spin-down occurs for mass outflow through the upper boundary — which corresponds, e.g., to the case of stellar wind mass loss from a convective envelope (cf. also Langer 1998) —, while a spin-up results from mass outflow through the lower boundary (cf. Fig. 1).

The latter situation is found in evolutionary models of a rotating $12\,\mathrm{M}_\odot$ star at the transition from the Hayashi-line to the blue supergiant stage. The star increased its rotational velocity one order of magnitude above the velocity which would result in the case of local angular momentum conservation. It would have increased its rotational velocity even further if it would not have arrived at critical rotation (cf. Sect. 3.2, Fig. 7), with the consequence of strong mass and angular momentum loss. At this point, the specific angular momentum loss $\dot{J}/\dot{M}$ reached about $8\,10^{19}\,\mathrm{cm}^2\,\mathrm{s}^{-1}$ (cf. Fig. 6).

The geometry of circumstellar matter around stars which undergo a red $\rightarrow$ blue transition may be strongly affected by the spin-up. We propose that this was the case for the progenitor of SN 1987A, the only star of which we know that it performed a red $\rightarrow$ blue transition in the recent past. The blue supergiant in its neighborhood studied by Brandner et al. (1997), around which they found a ring nebula as well, is another candidate. Also, B[e] stars may be related with the post-red supergiant spin-up (cf. Sect. 4.1). Furthermore, the spin-up mechanism studied in this paper may be relevant for bipolar outflows from central stars of proto-planetary nebulae (Sect. 4.4), from stars in the transition phase from the red supergiant stage to the Wolf-Rayet stage (Sect. 4.2), and from pre-main sequence stars (Sect. 4.3).

Acknowledgements. We are grateful to S.E. Woosley and S.P. Owocki for helpful discussions, to J. Fliegner for providing us with an implementation of rotational physics in the stellar evolution code, and to A. Weiss for supplying us with his recent opacity tables. This work has been supported by the Deutsche Forschungsgemeinschaft through grant No. La 587/15-1.

References

Alexander, D.R. 1994, BAAS, 184, #55.10
Antia, H.M., Basu, S., Chitre, S.M. 1997, MNRAS, submitted
Arnett, W.D., Bahcall, J.N., Kirshner, R.P., Woosley, S.E. 1989, ARAA 27, 629

Brandner, W., Grebel, E.K., Chu, Y.-H., Weis, K. 1997, ApJ, 457, L45
Bjorkman, J.E., Cassinelli, J.P. 1993, ApJ, 409, 429
Burrows, C.J., et al. 1995, ApJ, 452, 680
Chaboyer, B., Zahn, J.-P. 1992, A&A 253, 173
Chevalier, R.A. 1996, Ap&SS, 245, 255
Endal, A.S., Sofia, S. 1979, ApJ, 232, 531
Fliegner, J., Langer, N., Venn, K. 1996, A&A, 308, L13
Friend, D.B., Abbott, D.C. 1986, ApJ, 311, 701
Fukuda, I. 1982, PASP, 94, 271
García-Segura, G., Mac Low, M.-M. 1995, ApJ, 455, 160
García-Segura, G., Langer, N., Mac Low, M.-M. 1996, A&A, 316, 133
García-Segura, G., Langer, N., Różyczka, M., Franco, J. 1998, in preparation
Grevesse, N., Noels, A. 1993, in Origin and Evolution of the Elements, ed. N. Prantzo, E. Vangioni-Flam, M. Casse (Cambridge: Cambridge Univ. Press), 15
Gummersbach, C.A., Zickgraf, F.-J., Wolf, B. 1995, A&A, 302, 409
Halbedel, E.M. 1996, PASP, 108, 833
Heger, A., Jeannin, L., Langer, N., Baraffe, I. 1997, A&A, 327, 224
Ignace, R., Cassinelli, J.P., Bjorkman, J.E. 1996, ApJ, 459, 671
Iglesias, C.A., Rogers, F.J. 1996, ApJ, 464, 943
Koerner, W.D., Sargent, A.I. 1995, A.J., 109, 2138
Krishnamurthi, A., Pinsonneault, M.H., Barnes, S., Sofia, S. 1997, ApJ, 480, 303
Kumar, P., Narayan, R., Loeb, A. 1995, ApJ, 453, 480
Kwok, S. 1993, ARAA 31, 63
Lamers, H.J.G.M.L. 1993, in: Massive Stars: Their Lives in the Interstellar Medium, ed. J.P. Cassinelli, E.B. Churchwell, ASP Conf. Series, 35, 517
Langer, N. 1991a, A&A, 252, 669
Langer, N. 1991b, A&A, 243, 155
Langer, N. 1997, in: Luminous Blue Variables: Massive Stars in Transition, ed. A. Nota, H.J.G.L.M. Lamers., ASP Conf. Series, 120, 83
Langer, N. 1998, A&A, 329, 551
Langer, N., Heger A., 1998, in proc. of Worshop on B[e] stars, C. Jaschek and A.M. Hubert, eds., Kluwer, in press
Langer, N., Sugimoto, D., Fricke, K.J. 1983, A&A, 126, 207
Langer, N., Kiriakidis, M., El Eid, M.F., Frick, K.J., Weiss, A. 1988, A&A, 192, 177
Langer, N., García-Segura, G., Mac Low, M.-M. 1998, ApJ, submitted
Marti, J., Rodriguez, L.F., Reipurth, B. 1993, ApJ, 416, 208
Martin, C.L., Arnett, D. 1995, ApJ, 447, 378
Meyer, F. 1997, MNRAS, 285, L11
Meynet, G., Maeder, A. 1997, A&A, 321, 465
Nieuwenhuijzen, H., de Jager, C. 1990, A&A, 231, 134
Nota, A., Livio, M., Clampin, M., Schulte-Ladbeck, R. 1995, ApJ, 448, 788
Oudmaijer, R.D., Geballe, T.R., Waters, L.B.F.M., Sahu, K.C. 1994, A&A, 281, L33
Owocki, S.P., Cranmer, S.R., Gayley, K.G. 1996, ApJ, 472, L151
Owocki, S.P., Gayley, K.G. 1997, in: Luminous Blue Variables: Massive Stars in Transition, Eds. A. Nota, H.J.G.L.M. Lamers., ASP Conf. Series, 120, 121
Palla, F., Stahler, S.W. 1991, ApJ, 375, 288
Pinsonneault, M.H., Kawaler, S.D., Sofia, S., Demarque, P. 1989, ApJ, 338, 424
Pinsonneault, M.H., Deliyannis, C.P., Demarque, P. 1991, ApJ, 367, 239
Plait, P.C., Lundquist, P., Chevalier, R.A., Kirshner, R.P. 1995, ApJ, 439, 730
Podsiadlowski, Ph., 1998, in: SN 1987A: Ten years after, Fifth CTIO/ESO/LCO Workshop, ed. M.M. Phillips, N.B. Suntzeff, A.S.P. Conf. Series, in press
Schaller, G., Schaerer, D., Meynet, G., Maeder, A. 1992, A&AS, 96, 269
Schwarz, H.E., Corradi, R.L.M., Melnick, J. 1992, A&AS, 96, 23
Soker, N. 1996, ApJ, 460, L53
Spruit, H.C. 1998, A&A, submitted
Stanghellini, L., Corradi, R.L.M., Schwarz, H.E. 1993, A&A, 276, 463
Talon, S., Zahn, J.-P., Maeder, A., Meynet, G. 1997, A&A, 322, 209
Thompson, M.J., et al. 1996, Sci, 272, 1300
Walker, M.F. 1990, PASP 102, 726
Weaver, T.A., Zimmerman, G.B., Woosley, S.E. 1978, ApJ, 225, 1021
Woosley, S.E., Heger, A., Weaver, T.A., Langer, N. 1998, in: SN 1987A: Ten years after, Fifth CTIO/ESO/LCO Workshop, ed. M.M. Phillips, N.B. Suntzeff, A.S.P. Conf. Series, in press
Zahn, J.-P. 1974, in: Stellar Instability and Evolution, ed. P. Ledoux, A. Noels, A.W. Rogers IAU Symp., 59, 185
Zahn, J.-P. 1994, in: Evolution of Massive Stars: A Confrontation between Theory and Observation, ed. D. Vanbeveren, et al., (Dortrecht: Kluwer), p. 285
von Zeipel, H. 1924, MNRAS, 84, 665
Zickgraf, F.J., Humphreys, R.M., Lamers, H.J.G.L.M., Smolinski, J., Wolf, B., Stahl, O. 1996, A&A, 315, 510